Analytical Modeling of Three-Dimensional Temperature Distribution of Selective Laser Melting of Ti-6Al-4V

Jinqiang Ning* and Steven Y. Liang

George W. Woodruff School of Mechanical Engineering, Georgia Institute of Technology, 801 Ferst Drive, Atlanta, GA, USA, 30332-0405

* Author to whom correspondence should be addressed.

Abstract

Selective laser melting (SLM) is one of the widely used techniques in metallic additive manufacturing, in which high-density laser powder is utilized to selectively melting layers of powders to create geometrically complex parts. Temperature distribution and molten pool geometry directly determine the balling effect, and concentrated balling phenomenon significantly deteriorates surface integrity and mechanical properties of the part. Finite element models have been developed to predict temperature distribution and molten pool geometry, but they were computationally expensive. In this paper, the three-dimensional temperature distributions are predicted by analytical models using point moving heat source and semi-ellipsoidal moving source respectively. The molten pool dimensions under various process conditions are obtained from the three-dimensional temperature predictions and experimentally validated. Ti-6Al-4V alloy is chosen for the investigation. Good agreements between the predictions and the measurements are observed. The presented models are also suitable for other metallic materials in the SLM process.

Keywords: Metallic Additive Manufacturing, Selective Laser Melting, Analytical Modeling, 3D Temperature Prediction, Molten Pool Dimension.

 doi:10.20944/preprints201809.0101.v1

Introduction

Additive manufacturing (AM), alternatively named 3D printing, has been extensively studied in the past two decades. AM process is a cost-effective process for a single part or small batches, and it is capable of producing geometrical complex parts [1]. Selective laser melting (SLM) is widely used in metallic additive manufacturing, in which a high-density laser powder is utilized to fully melting layers of powders to create geometrically complex parts. However, consistency of the part quality for batch production is difficult to control due to intense heat input and repeatedly rapid melting and solidification. Problems such as balling effect, deteriorated surface finish, undesired residual stress and part distortion have been frequently observed in the SLM process. It has been reported that the process parameters such as laser power and scanning speed have considerable influence on the molten pool geometry, and the molten pool geometry directly determines the balling effect and thus affects surface integrity [2]. A large molten pool length to width ratio ($L/W > \pi$) indicates that balling effect is at the concentrated condition. The balls form in various shapes due to the inadequate energy input or the molten pool splashing under high scan speed [3]. Balling effect at concentrated conditions considerably deteriorates the surface roughness. A post-processing procedure such as polishing becomes necessary and thus decreases the dimensional accuracy. In addition, a large number of pores tends to be formed due to the discontinuity of the formed balls, resulting in poor mechanical properties [4].

Numerical analyses based on finite element analysis (FEA) and analytical models have been developed to investigate temperature distribution in the SLM process.

Different processing techniques have been applied in FEA simulation to predicted temperature distribution. Peyre P. *et al.* developed a FEA model using steady-state calculations to predict temperature distribution and molten pool geometry in printing a thin wall structure using a laser-based direct metal deposition process [5]. Paul S. *et al.* developed another FEA model to predict the temperature distribution and molten pool geometry using element birth technique with uniform moving heat source and Gaussian powder distribution. Other multiple-physics numerical models have also been developed to predict the temperature distribution and molten pool

Preprints (www.preprints.org) | NOT PEER-REVIEWED | Posted: 5 September 2018 doi:10.20944/preprints201809.0101.v1

geometry [6-10]. Although the developed FEA models have made considerable progress in predicting temperature distribution and molten pool geometry in AM processes, the expensively computational cost and time are still the main drawbacks.

Analytical models have also been developed to predict temperature distribution using closed-form solutions. Li JF *et al.* developed an analytical model with the Green function method to predict the temperature distribution with a volumetric heat source and surface heat source respectively [11]. The hydrodynamics of the molten pool is neglected by implementing proper volume heat flux. Batut B. *et al*. developed another analytical model to predict two-dimensional temperature distribution using modified point moving heat source solution with arbitrarily shaped laser source [12]. Fergani O. *et al.* also presented an analytical model to predict two-dimensional temperature distribution using point moving heat source [13]. Isotropic and homogeneous material and semi-infinite medium were assumed in the analytical model. Li's model has demonstrated the capability of three-dimensional temperature prediction in AM process, but the integrated Green function dramatically increased the mathematical complexity and resulting in a decreased computational efficiency. Batut's models and Fergani's model only predicted two-dimensional temperature distributions in AM process.

In this work, three-dimensional temperature distributions under varying process conditions in SLM are predicted by two analytical models. A point moving heat source and a semi-ellipsoidal heat source are used in the two analytical models respectively. Molten pool dimensions are obtained from the predicted three-dimensional temperature distribution under each process condition. The predicted molten pool dimensions including melting length, melting depth, and melting width are validated with experimental measurements adopted from literature.

Materials and Method

In this paper, the three-dimensional temperature distributions in SLM of Ti-6Al-4V under varying process conditions are investigated by analytical models. The temperature profile near the moving heat source in a single-track scanning was predicted by two analytical models separately. One analytical model uses a point moving heat source assumption; the other analytical model uses a three-

Preprints (www.preprints.org) | NOT PEER-REVIEWED | Posted: 5 September 2018 doi:10.20944/preprints201809.0101.v1

dimensional semi-ellipsoidal moving heat source assumption. In addition, the medium is assumed to be isotropic, homogeneous, and semi-infinite in the analytical models. The materials properties are temperature-dependent and adopted as they are at room temperature as given in Table 1.

Table 1. Physical and thermal properties of Ti-6Al-4V [14,15]

Density (Kg/m3)	4428
Specific heat (J/Kg-K)	580
Thermal conductivity (W/m-K)	7.2
Room temperature (°C)	25
Melting Temperature (°C)	1655
Evaporation Temperature (°C)	2976

The molten pool dimensions are determined based on the comparison between predicted temperature distribution and melting temperature. A typical molten pool geometry in SLM is illustrated in Figure 1. The melting length (L), melting width (W) and melting depth (D) are the greatest lengths along the heat source moving direction (x-axis), transverse direction (y-axis), and in-depth direction (z-axis) respectively.

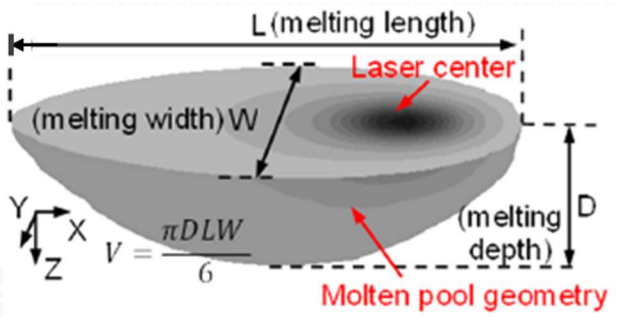

Figure 1. Schematic drawing of a molten pool in SLM process. Laser travels along x-direction [11].

Moreover, varying laser power magnitudes are used in the predictions to investigate the influence of laser power on the molten pool size. The laser is continuous at the wavelength ($\lambda = 1.06\ \mu m$) that is typical in the SLM process. The energy absorption coefficient of Ti-6Al-4V powder is assumed to be the same as pure titanium powder, given as 0.77 [16]. The process parameters in SLM are given in Table 2.

Table 2. Process parameters [17]

Laser Type	Nd: YAG laser
Laser Power (W)	20-80
Scanning Speed (mm/s)	200
Laser spot radius (μm)	26

Preprints (www.preprints.org) | NOT PEER-REVIEWED | Posted: 5 September 2018 doi:10.20944/preprints201809.0101.v1

The general convection-diffusion equation can be expressed as

$$\frac{\partial \rho u}{\partial t} + \frac{\partial \rho h V}{\partial x} = \nabla \cdot (k \nabla T) + \dot{q} \quad (1)$$

where u is internal energy, h is enthalpy, ρ is density, k is conductivity, and $\dot{q}$ is a volumetric heat source, t is time, V is heat source moving speed, and T is temperature.

When $V = 0$, the Equation (1) becomes the heat conduction equation. The heat conduction can be expressed as the following with $du = c\, dT$, where c is heat capacity.

$$c \frac{\partial \rho T}{\partial t} = \nabla \cdot (k \nabla T) + \dot{q} \quad (2)$$

The steady state equation with constant velocity can be simplified using the continuity equation. The continuity equation is expressed as

$$\frac{\partial \rho}{\partial t} + \frac{\partial \rho V}{\partial x} = 0 \quad (3)$$

The heat conduction equation then becomes

$$\rho c(T) V \frac{\partial T}{\partial x} = \nabla \cdot (k(T) \nabla T) + \dot{q} \quad (4)$$

The heat conduction equation can be solved with assumptions of a point moving heat source and a semi-ellipsoidal moving heat source for isotopic and semi-infinite medium [18].

Point Moving Heat Source

A point moving heat source solution for the temperature field in a three-dimensional semi-infinite body is presented by Carslaw and Jaeger [19]. The solution is expressed as

$$\theta = \frac{P}{4\pi\kappa R(T_m - T_0)} \exp\left(\frac{-V(R + x)}{2\kappa}\right) \quad (5)$$

where θ is the dimensionless temperature, κ is thermal diffusivity, R is the distance from the heat source location. They are defined as the following:

$$\theta = \frac{T - T_0}{T_m - T_0}$$

$$\kappa = \frac{k}{\rho c}$$

$$R^2 = x^2 + y^2 + z^2$$

Semi-ellipsoidal Moving Heat Source

A moving heat source solution in a three-dimensional semi-infinite body with a three-dimensional semi-ellipsoidal heat source was developed by Nguyen [20]. This solution is expressed as

$$\theta = \frac{1}{\sqrt{2\pi}} \int_0^{\frac{V^2 t}{2\kappa}} \frac{d\tau}{\sqrt{(\tau + {u_a}^2)}\sqrt{\tau + {u_b}^2}} \left(\frac{A_1}{\sqrt{\tau + {u_c}^2}}\right)$$

Preprints (www.preprints.org) | NOT PEER-REVIEWED | Posted: 5 September 2018 doi:10.20944/preprints201809.0101.v1

(6)

Where

$$A_1 = \exp\left(-\frac{(\xi+\tau)^2}{2(\tau+{u_c}^2)} - \frac{\psi^2}{2(\tau+{u_b}^2)} - \frac{\zeta^2}{2(\tau+{u_b}^2)}\right)$$

$$\xi = \frac{Vx}{2\kappa}; \psi = \frac{Vy}{2\kappa}; \zeta = \frac{Vz}{2\kappa};\ \tau = \frac{V^2(t-t')}{2\kappa};$$

$$u_a = Va_h 2\sqrt{6\kappa}; u_b = Vb_h 2\sqrt{6\kappa}; u_c = Vc_h 2\sqrt{6\kappa};$$

$$n = \frac{PV}{4\pi\kappa^2\rho C_p(T_m - T_0)}$$

where a_h, b_h, c_h are heat source parameters. a_h and c_h are assumed to be the same as laser spot radius. b_h is obtained based on the given heat flux at given heat source location using the following equation, given as 7.6 μm.

$$\dot{q} = \frac{6\sqrt{3}P}{a_h b_h c_h \pi\sqrt{\pi}} \exp\left(-\frac{3x^2}{{c_h}^2} - \frac{3y^2}{{a_h}^2} - \frac{3z^2}{{b_h}^2}\right)$$

(7)

Results and Discussion

Three-dimensional temperature profiles in SLM of Ti-6Al-4V were predicted by analytical models using point moving heat source and semi-ellipsoidal moving heat source respectively. The temperature profiles on the top surface and cross sections at heat source location were plotted to illustrate the molten pool geometry and heat affected zone due to a single-track scanning. The molten pool geometry was determined as space where predicted temperatures were higher than melting temperature. Molten pool length, width, and depth were obtained from the three-dimensional temperature profile. The molten pool width and depth were validated by experimental measurements. The experimental measurements were adopted from literature, in which the molten pool size was measured by optical microscopy based on the solidified structure [17].

The three-dimensional temperature profiles predicted with the analytical model using point moving heat source are shown in Figure 1. Isotropic and homogeneous material and semi-infinite body are assumed in the prediction. The laser power and scanning speed are 20 W and 200 mm/s respectively. Laser travels along the x-direction. Isothermal lines are plotted at temperature levels of 30, 100, 500,1000, and 1655 in Celsius.

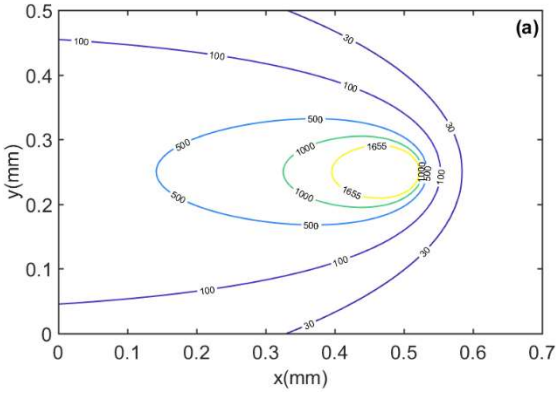

Preprints (www.preprints.org) | NOT PEER-REVIEWED | Posted: 5 September 2018 doi:10.20944/preprints201809.0101.v1

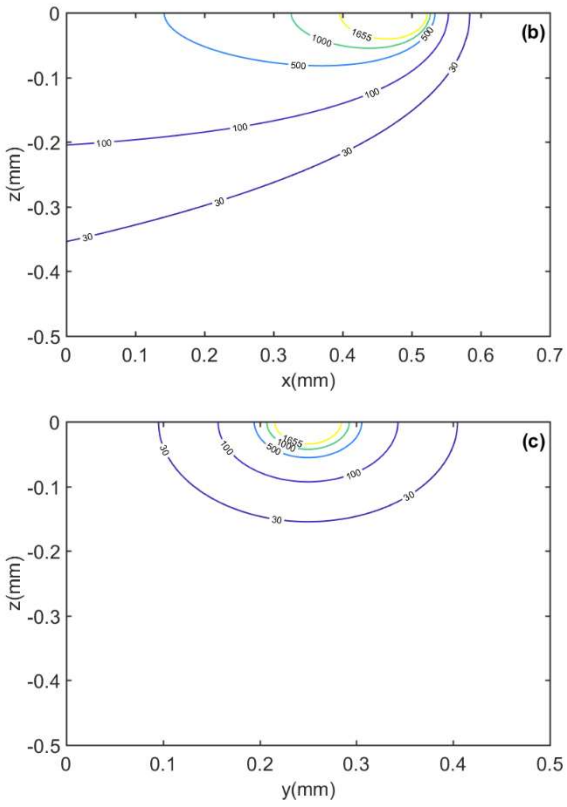

Figure 2. Temperature profile using point moving heat source with P = 20 w, V = 200mm/s. The temperature profile in top view (a), front view of the cross-section (b), right view of the cross-section. Note cross sections are at heat source location. Heat source moves along the x-direction.

The three-dimensional temperature profiles predicted with an analytical model using a semi-ellipsoidal moving heat source are shown in Figure 3. Same laser power and scanning speed are used in the prediction. Isothermal lines are plotted at temperature levels of 30, 100, 500,1000, and 1655 in Celsius.

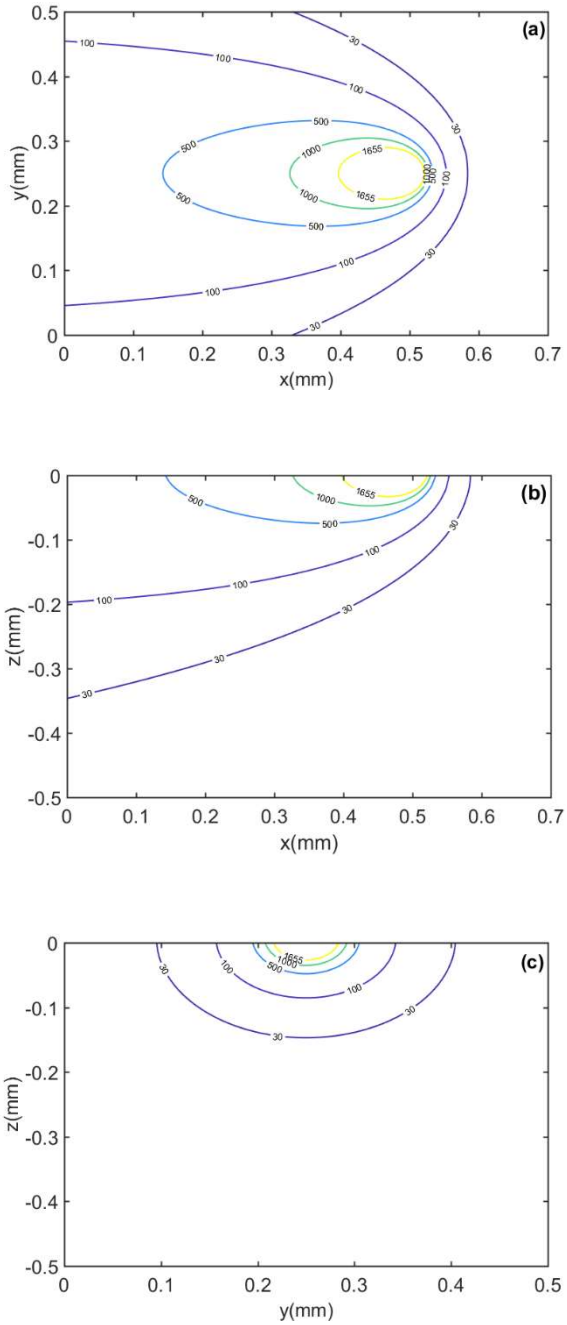

Figure 3. Temperature profile using semi-ellipsoidal moving heat source with P = 20 w, V = 200mm/s. The temperature profile in top view (a), front view of the cross-section (b), right view of the cross-section. Note

Preprints (www.preprints.org) | NOT PEER-REVIEWED | Posted: 5 September 2018 doi:10.20944/preprints201809.0101.v1

cross sections are at heat source location. Heat source moves along the x-direction.

The predicted temperature profiles by analytical models with two types of heat source are in excellent agreements. However, the molten pool dimensional analysis indicates that the predicted temperatures using point heat source are slightly larger than the prediction using a semi-ellipsoidal heat source, resulting in a slightly larger molten pool size, which confirms the institutive trend that the more concentrated laser powder, the high peak temperature and the larger the molten pool. In addition, the temperature prediction as heat source location using point moving heat source becomes infinite based on the mathematical equation (5), which also confirms the institutive trend.

The temperature predictions were then conducted under different process conditions, specifically with laser power at 20 W, 40 W, 60W and 80W. The molten pool length, width, and depth were obtained from the three-dimensional temperature predictions under each process condition. The molten pool volume was calculated as $V = \frac{\pi DLW}{6}$, given L, W, D are the molten pool length, width and depth respectively. The results using two analytical models and experimental results are shown in Figure 4. Good agreements were observed between the predicted molten pool dimensions and the experimental measurements. Positive correlations were observed between input laser powder and molten pool depth, width, length, and volume, which agrees with experimental measurements. In addition, the molten pool length to width ratios were less than π, which indicated no balling effect at concerned condition [2]. This finding agrees with the conclusion in the literature [17].

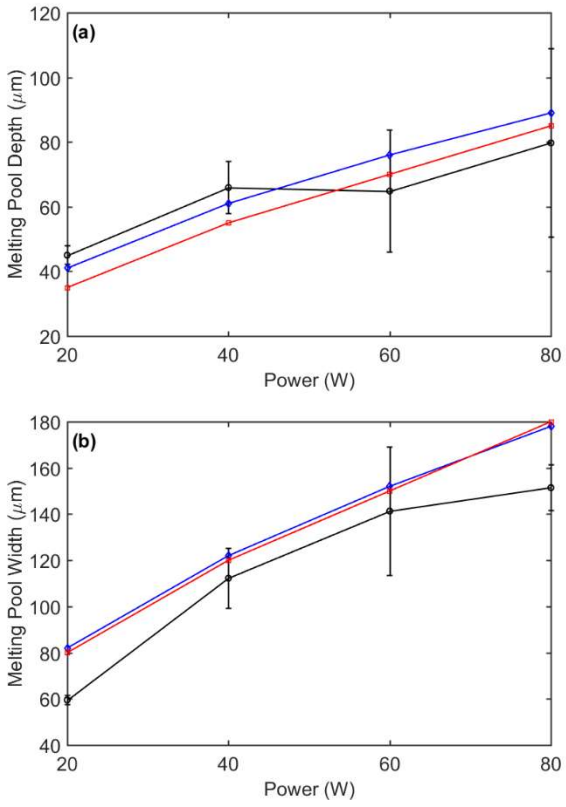

Preprints (www.preprints.org) | NOT PEER-REVIEWED | Posted: 5 September 2018 doi:10.20944/preprints201809.0101.v1

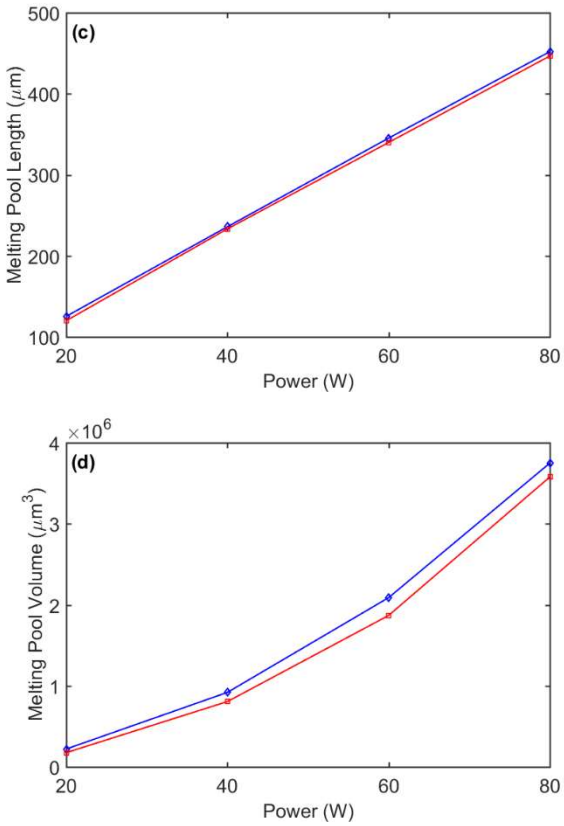

Figure 4. Predicted molten pool dimensions and experimental measurements under varying process conditions. (a) molten pool depth, (b) molten pool width, (c) molten pool length, (d) molten pool volume.

Conclusion

This paper presents analytical models using two types of heat sources, namely point moving heat source and semi-ellipsoidal moving heat source, to predict the three-dimensional temperature distribution in the SLM process. The prediction temperature profiles under the same process condition using two heat sources agree well. The slightly larger temperatures predicted with the point moving heat source is observed due to the more concentrated power input of point heat source. The predicted molten pool geometry specifically melting depth and melting width closely agree with the experimental measurements under varying process conditions. In addition, the increasing molten pool size is observed with increasing laser power input. The presented analytical models can also predict temperature distribution and molten pool geometry for other metallic materials in SLM. In the future, the heat loss due to convection and radiation on the top surface of the medium needs to be considered. The heat conduction solutions using in work are linear and thus the temperature prediction of multiple heat sources can be obtained as a combination of elementary heat sources.

Author Disclosure Statements

No competing financial interests exist.

References

1. Levy GN, Schindel R, Kruth JP. Rapid manufacturing and rapid tooling with layer manufacturing (LM) technologies, state of the art and future perspectives. CIRP Ann-Manuf Technol. 2003;52(2):589-609.
2. Kruth JP, Levy G, Klocke F, Childs TH. Consolidation phenomena in laser and powder-bed based layered manufacturing. CIRP Ann. 2007;56(2):730-759.
3. Gu DD, Shen YF. Balling phenomena in direct laser sintering of stainless steel powder: metallurgical mechanisms and control methods. Mater Design. 2009; 30(8):2903–2910.
4. Li R, Liu J, Shi Y, Wang L, et al. Balling behavior of stainless steel and nickel powder during selective laser melting process. Int J Adv Manuf Technol. 2012; 59(9-12):1025-1035.
5. Peyre P, Aubry P, Fabbro R, et al. Analytical and numerical modelling of the direct metal deposition laser process. J of Phys D: Appl Phys. 2008; 41(2):025403.
6. Paul S, Singh R, Yan W. Thermal model for additive restoration of mold steels using crucible steel. J of Manuf Process. 2016; 24:346-354.
7. Parekh R, Buddu RK, Patel RI. Multiphysics simulation of laser cladding process to study the effect of process parameters on clad geometry. Procedia Technol. 2016; 23:529-536.
8. Vásquez F, Ramos-Grez JA, Walczak M. Multiphysics simulation of laser–material interaction during laser powder deposition. The Int J Adv Manuf Technol. 2012; 59(9-12):1037-1045.
9. Kumar A, Roy S. Effect of three-dimensional melt pool convection on process characteristics during laser cladding. Comput Mater Sci. 2009; 46(2):495-506.
10. Morville S, Carin M, Peyre P, Gharbi M, et al. 2D longitudinal modeling of heat transfer and fluid flow during multilayered direct laser metal deposition process. J Laser Appl. 2012; 24(3):032008.
11. Li JF, Li L, Stott FH. Comparison of volumetric and surface heating sources in the modeling of laser melting of ceramic materials. Int J Heat Mass Transf. 2004; 47(6-7):1159-1174.
12. de La Batut B, Fergani O, Brotan V, et al. Analytical and numerical temperature prediction in direct metal deposition of Ti6Al4V. J Manuf Mater Process. 2017; 1(1):3.

13. Fergani O, Berto F, Welo T, et al. Analytical modelling of residual stress in additive manufacturing. Fatigue Fract Eng Mater Struct. 2017; 40(6):971-978.
14. Boyer R, Collings E. Materials Properties Handbook: Titanium Alloys. Materials Park, OH: ASM International,1993.
15. Boivineau M, Cagran C, Doytier D, et al. Thermophysical properties of solid and liquid Ti-6Al-4V alloy. Int J Thermophys. 2006; 27(2):507-529.
16. Tolochko NK, Khlopkov YV, Mozzharov S E, et al. Absorptance of Powder Materials Suitable for Laser Sintering. Rapid Prototyping J. 2000; 6(3):155–161.
17. Fu CH, Guo YB. Three-dimensional temperature gradient mechanism in selective laser melting of Ti-6Al-4V. J Manuf Sci and Eng. 2014; 136(6):061004.
18. Van Elsen M, Baelmans M, Mercelis P, et al. Solutions for modelling moving heat sources in a semi-infinite medium and applications to laser material processing. Int J Heat Mass Transf. 2007; 50(23-24):4872-4882.
19. Carslaw H, Jaeger J. Conduction of Heat in Solids. Oxford: Oxford Science Publication,1990.
20. Nguyen NT, Ohta A, Matsuoka K, et al. Analytical solutions for transient temperature of semi-infinite body subjected to 3-D moving heat sources. Weld Res Suppl. 1999; 78:265-274.